ISSN 1674-1056
http://cpb.iphy.ac.cn
http://iopscience.iop.org/cpb
中国物理 B
Chinese Physics
中国物理 Chinese Physics B

Superconductivity with peculiar upper critical fields in quasi-one-dimensional Cr-based pnictides

Guang-Han Cao(曹光旱), Zeng-Wei Zhu(朱增伟)

Citation: Chin. Phys. B . 2018, 27(10): 107401. **doi:** 10.1088/1674-1056/27/10/107401

Journal homepage: http://cpb.iphy.ac.cn; http://iopscience.iop.org/cpb

What follows is a list of articles you may be interested in

Nonlinear uniaxial pressure dependence of the resistivity in $Sr_{1-x}Ba_xFe_{1.97}Ni_{0.03}As_2$

Hui-Can Mao(毛慧灿), Dong-Liang Gong(龚冬良), Xiao-Yan Ma(马肖燕), Hui-Qian Luo(罗会仟), Yi-Feng Yang(杨义峰), Lei Shan(单磊), Shi-Liang Li(李世亮)

Chin. Phys. B . 2018, 27(8): 087402. **doi:** 10.1088/1674-1056/27/8/087402

Effect of Mn substitution on superconductivity in iron selenide (Li, Fe)OHFeSe single crystals

Yiyuan Mao(毛义元), Zian Li(李子安), Huaxue Zhou(周花雪), Mingwei Ma(马明伟), Ke Chai(柴可), Shunli Ni(倪顺利), Shaobo Liu(刘少博), Jinpeng Tian(田金鹏), Yulong Huang(黄裕龙), Jie Yuan(袁洁), Fang Zhou(周放), Jianqi Li(李建奇), Kui Jin(金魁), Xiaoli Dong(董晓莉), Zhongxian Zhao(赵忠贤)

Chin. Phys. B . 2018, 27(7): 077405. **doi:** 10.1088/1674-1056/27/7/077405

Distinction between critical current effects and intrinsic anomalies in the point-contact Andreev reflection spectra of unconventional superconductors

Ge He(何格), Zhong-Xu Wei(魏忠旭), Jérémy Brisbois, Yan-Li Jia(贾艳丽), Yu-Long Huang(黄裕龙), Hua-Xue Zhou(周花雪), Shun-Li Ni(倪顺利), Alejandro V Silhanek, Lei Shan(单磊), Bei-Yi Zhu(朱北沂), Jie Yuan(袁洁), Xiao-Li Dong(董晓莉), Fang Zhou(周放), Zhong-Xian Zhao(赵忠贤), Kui Jin(金魁)

Chin. Phys. B . 2018, 27(4): 047403. **doi:** 10.1088/1674-1056/27/4/047403

Controlled synthesis of ferromagnetic $MnSe_x$ particles

Junjie Sun(孙俊杰), Chao Li(李超), Duo Chen(陈铎), Shishou Kang(康仕寿), Guolei Liu(刘国磊), Shuyun Yu(于淑云), Guangbing Han(韩广兵), Liangmo Mei(梅良模)

Chin. Phys. B . 2016, 25(10): 107405. **doi:** 10.1088/1674-1056/25/10/107405

Hybrid crystals of cuprates and iron-based superconductors

Xia Dai(代霞), Cong-Cong Le(勒聪聪), Xian-Xin Wu(吴贤新), Jiang-Ping Hu(胡江平)

Chin. Phys. B . 2016, 25(7): 077402. **doi:** 10.1088/1674-1056/25/7/077402

TOPICAL REVIEW — Fundamental research under high magnetic fields

Superconductivity with peculiar upper critical fields in quasi-one-dimensional Cr-based pnictides*

Guang-Han Cao(曹光旱)[1,†] and Zeng-Wei Zhu(朱增伟)[2]

[1] Department of Physics, Zhejiang University, Hangzhou 310027, China

[2] Wuhan National High Magnetic Field Center, School of Physics, Huazhong University of Science and Technology, Wuhan 430074, China

(Received 20 June 2018; revised manuscript received 19 July 2018; published online 10 September 2018)

The discovery of superconductivity in quasi-one-dimensional Cr-based pnictides $A_2Cr_3As_3$ (A = alkali metals) has generated considerable research interest, primarily owing to their reduced dimensionality, significant electron correlations, and possible unconventional superconductivity. The upper critical field (H_{c2}) provides important information on the superconducting pairing. In this paper, we first briefly overview the latest research progress on the Cr-based superconductors. Then, we introduce typical $H_{c2}(T)$ behaviors of type-II superconductors in relation with the pair-breaking mechanisms. After a description of the measurement method for H_{c2}, we focus on the analysis of H_{c2} data, especially for the temperature and angle dependence, in $K_2Cr_3As_3$ crystals. The result indicates (i) an absence of Pauli-paramagnetic pair breaking for field perpendicular to the Cr_3As_3 chains, and (ii) a unique threefold modulation for the in-plane $H_{c2}(\phi)$ profile. Finally we conclude with remarks on the possible unconventional superconducting pairing symmetry.

Keywords: Cr-based superconductors, upper critical fields, unconventional superconductivity

PACS: 74.70.Xa, 74.10.+v, 74.25.Op **DOI:** 10.1088/1674-1056/27/10/107401

1. Introduction

Superconductivity is an intriguing macroscopic quantum state in solids due to the condensation of electronic Cooper pairs. In a phonon-mediated BCS-type conventional superconductor, the superconducting order parameter is mostly of an s-wave in which the underlying Cooper pairs are in a spin-singlet state. In a so-called unconventional superconductor, however, the electron pairing interaction is basically non-phonon-mediated and, the superconducting order parameter is mostly of a non-s-wave, which breaks additional symmetries apart from the global $U(1)$ gauge symmetry.[1] If the Cooper pairs are of spin triplet, which is analogous to those in ^{3}He superfluid phases, the superconductor is always considered as being unconventional. Nonetheless, such a spin-triplet superconductor appears to be rare. Up to 2014, the main candidates of spin-triplet superconductors include some organic superconductors,[2,3] UPt_3,[4,5] Sr_2RuO_4,[6] and U-based superconducting ferromagnets.[7] Note that the superconducting transition temperature T_c of these superconductors is relatively low (below 1.5 K), which is undesirable for in-depth investigations.

Following the discovery of superconductivity at $\sim$ 2 K under an external pressure of $\sim$ 1 GPa in CrAs,[8,9] quasi-one-dimensional (Q1D) Cr-based arsenides $A_2Cr_3As_3$ (A = K, Rb, and Cs) were discovered in 2015.[10–14] The superconducting transition temperature T_c is 6.1, 4.8, and 2.2 K, respectively, for A = K, Rb, and Cs. The normal-state $\rho(T)$ behavior is very different for polycrystalline and single-crystalline samples, primarily because of the anisotropy (see below). The polycrystalline samples show somewhat linear temperature dependence of resistivity [Fig. 1(a)]. In contrast, for high-quality crystals of $K_2Cr_3As_3$, the normal-state $\rho(T)$ below 50 K follows a power-law relation with an exponent close to 3 [Fig. 1(b)]. The T_c value of high-quality crystals is also increased a little, compared with that of the polycrystalline samples. The defect/impurity effect on T_c can be seen elsewhere,[15] which shows substantial suppression of superconductivity due to nonmagnetic scattering, suggestive of a non-s-wave pairing in $K_2Cr_3As_3$.

Note that the T_c value increases monotonically with the decrease of ionic radii of the alkali-metal elements, which implies that T_c could be further increased if K^+ ions are replaced with smaller cations such as Na^+ and Li^+. Whereas high-temperature synthesis of these target compounds were unsuccessful,[14] very recently, it was reported that the expected sister compound $Na_2Cr_3As_3$ could be obtained through an ion-exchange process.[16] The T_c value was indeed increased (up to 8.6 K). This finding further corroborates that T_c increases with decreasing the a axis (interchain distance), as shown in Fig. 2. Interestingly, the Sommerfeld coefficient, derived from the specific-heat measurements, follows a similar dependence.[14]

*Project supported by the National Natural Science Foundation of China (Grant Nos. 11674281 and 11574097) and the Fundamental Research Funds for the Central Universities of China.

†Corresponding author. E-mail: ghcao@zju.edu.cn

© 2018 Chinese Physical Society and IOP Publishing Ltd

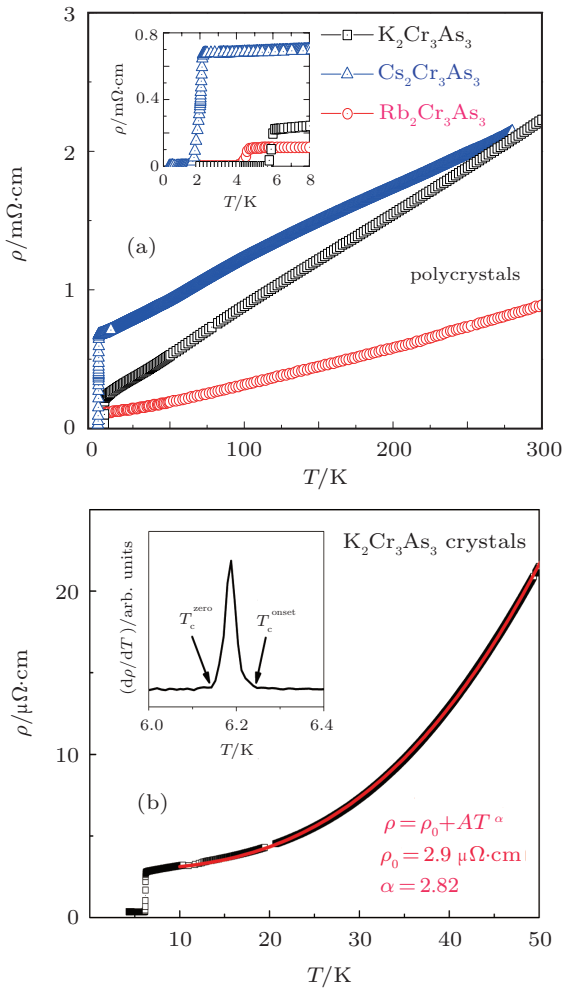


Fig. 1. (color online) (a) Resistive superconducting transitions in polycrystals of $A_2Cr_3As_3$ (A=K, Rb, Cs). The inset shows the close-up. (b) Superconducting transition in electrical resistivity (with current flowing along the c-axis direction) for $K_2Cr_3As_3$ single crystals. The inset shows the derivative of resistivity, defining $T_c^{onset} = 6.24$ K and $T_c^{zero} = 6.15$ K.

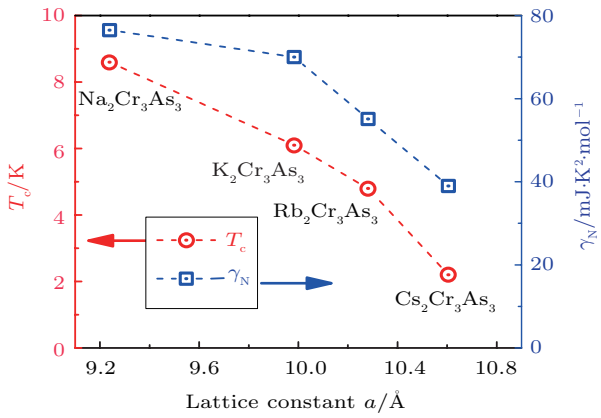


Fig. 2. (color online) Superconducting transition temperature T_c (left) and the electronic specific-heat coefficient γ_N (right) as functions of the lattice parameter a for $A_2Cr_3As_3$ (A =Na, K, Rb, Cs).

If the increase of T_c above is considered as a consequence of chemical pressure, then the effect of physical pressure is surprisingly in an opposite tendency. Earlier preliminary data show that T_c of $K_2Cr_3As_3$ decreases at a rate of -0.34 K/GPa under hydrostatic pressures up to 0.7 GPa.[17] Later high-pressure measurements together with crystal-structure investigations were done for both $K_2Cr_3As_3$ and $Rb_2Cr_3As_3$.[18] The result indicates that T_c decreases almost linearly to below 2 K and, by extrapolation, superconductivity disappears at about 8 GPa and 6 GPa, respectively, for $K_2Cr_3As_3$ and $Rb_2Cr_3As_3$. A similar result was independently reported for $K_2Cr_3As_3$.[19] *In-situ* structural determinations reveal that the extent of non-centrosymmetry, defined by the difference between bond angles of As2−Cr2−As2 (α) and As1−Cr1−As1 (β), seems to be in relation with superconductivity. Note that for the centrosymmetric non-superconducting 133 series ACr_3As_3 (A = K, Rb, Cs),[20,21] the $(\alpha - \beta)$ value becomes zero since there is only one Cr site.

Dramatically, Ren and co-workers[22] recently reported that the 133-type KCr_3As_3 could superconduct at 5 K provided it was in single crystalline form. Additionally, the same group observed superconductivity at 7.3 K in $RbCr_3As_3$ single crystals.[23] The T_c value of the latter case is significantly higher than that of $Rb_2Cr_3As_3$ (4.8 K), which basically rules out the possibility that superconductivity may come from $Rb_2Cr_3As_3$ that resides in the sample. So far, however, it is not clear whether $CsCr_3As_3$ and $NaCr_3As_3$ crystals superconduct or not.

Before ending this section, we introduce efforts on explorations of superconductivity in quasi-two-dimensional (Q2D) Cr-based systems. Actually, it was the attempt to look for superconductivity in "$Ba_{1-x}K_xCr_2As_2$" that led to the discovery of the Q1D $K_2Cr_3As_3$ superconductor.[14] Along this line, we also discovered $Sr_2Cr_3As_2O_2$[24] and $Ba_2Ti_2Cr_2As_4O$,[25] unfortunately, neither of them are superconducting above 1.8 K. Some theoretical studies predict that doped Q2D Cr-based pnictides could host unconventional superconductivity.[26,27] So far, however, we have not yet observed any trace of superconductivity in the Q2D systems.

2. Basic properties of $A_2Cr_3As_3$

As shown in Fig. 3(a), the $A_2Cr_3As_3$ family is structurally characterized by the $[(Cr_3As_3)^{2-}]_\infty$ double-walled linear subnanotubes separated by the K^+ counterions. Consistent with the Q1D crystal structure, the resistivity data [Fig. 3(b)] indeed show a strong anisotropy with an anisotropic ratio, $\gamma_\rho = \rho^{\|ab}(T)/\rho^{\|c}(T)$, up to 120 at 50 K. The $\rho^{\|ab}(T)$ shows a quasi-linear behavior below $\sim$ 30 K, which may account for the large resistivity value and linearity in polycrystalline samples [Fig. 1(a)]. At around 50 K, interestingly, $\rho^{\|ab}(T)$ exhibits a resistivity maximum, characteristic of 3D-to-1D dimension crossover as observed in Q1D so-called Bechgaard slats.[28] This result suggests that a Tomonaga–Luttinger liquid (TLL) state could be realized at high temperatures.[28,29]

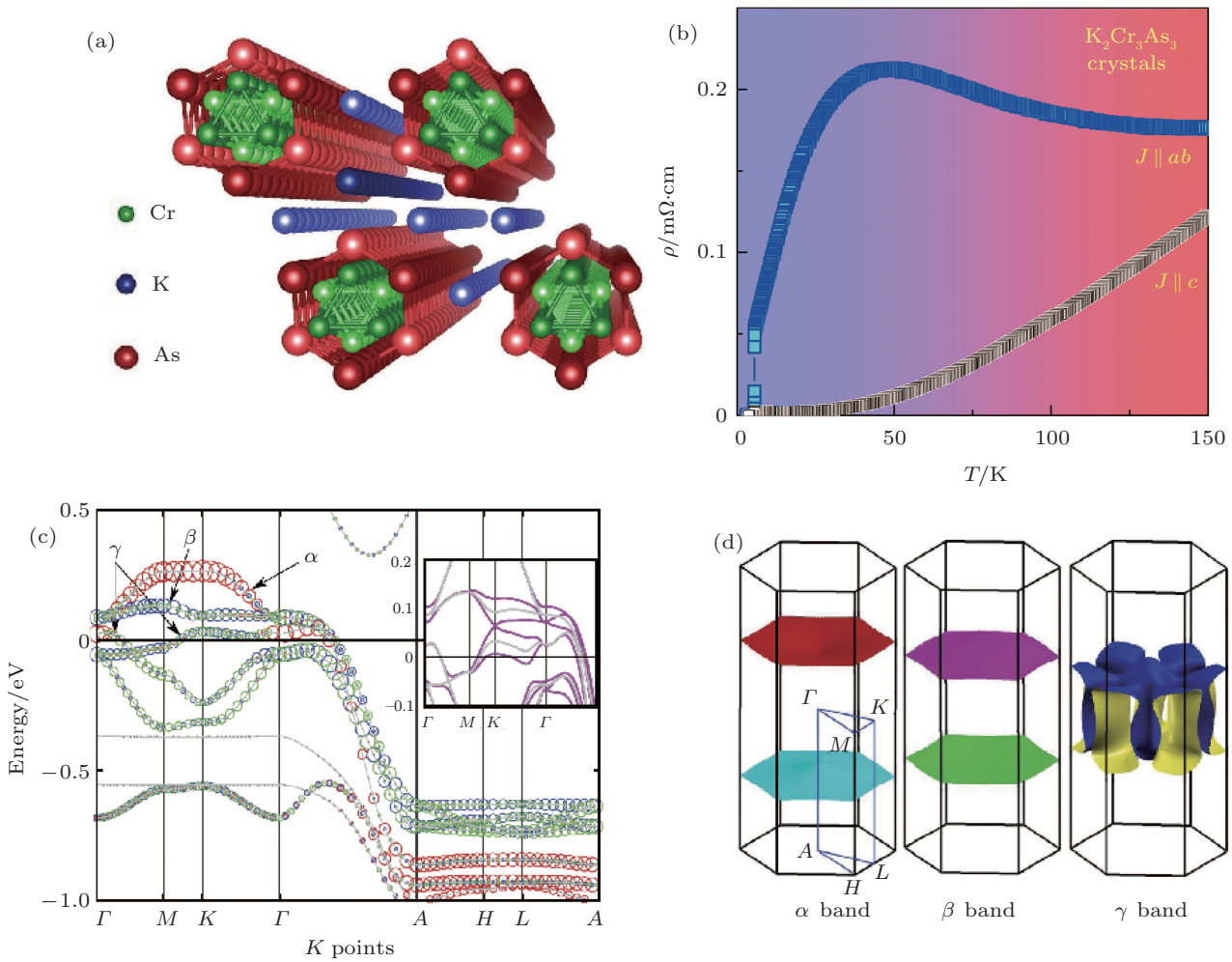


Fig. 3. (color online) (a) A top view of the crystal structure of $K_2Cr_3As_3$ with the c axis along the linear Cr_3As_3 chain. (b) Anisotropic resistivity of $K_2Cr_3As_3$ single crystals, from which a 3D-to-1D dimension crossover can be seen in the case of $J \| ab$ (i.e., electric current flowing perpendicular to the chain direction). (c) Calculated band structure of nonmagnetic $K_2Cr_3As_3$. The inset shows comparison between relativistic (in dark violet) and non-relativistic (in grey) results (from Ref. [30]). (d) Fermi-surface sheets (non-relativistic result).

The inner Cr_3 sub-nanotubes can be theoretically modelled in terms of a twisted Hubbard tube, which gives rise to 1D molecular-orbital bands.[31] Electronic band-structure calculations reveal that the electronic states near the Fermi energy are dominated by the Cr-3d atomic orbitals.[30] Note that the asymmetrical spin–orbit interactions are sizable around K and Γ points, as shown in the inset of Fig. 3(c). There are two Q1D Fermi-surface sheets (FSs) in the α and β bands and one three-dimensional (3D) FS pockets in the γ band [Fig. 3(d)].[30,32,33] The two hole-like Q1D FSs are experimentally observed in a recent angle-resolved photoemission spectroscopy study,[34] from which a TLL behavior is signatured. The TLL physics has been earlier suggested both experimentally[35] and theoretically.[31,36,37]

For the prototype compound $K_2Cr_3As_3$, the total density of states (DOS) at E_F is calculated to be $N(E_F) = 8.58\ \mathrm{eV}^{-1} \cdot \mathrm{fu}^{-1}$,[30] corresponding to a 'bare' electronic specific-heat coefficient of $20\ \mathrm{mJ \cdot K^{-2} \cdot mol^{-1}}$. The experimental Sommerfeld coefficient ($\gamma_N \sim 70\ \mathrm{mJ \cdot K^{-2} \cdot mol^{-1}}$) is 3.5 times larger,[10] indicating remarkable electron-mass renormalization (electron–phonon coupling constant is generally less than 1.0 owing to the lattice instability). Similar comparison between calculations and experiments for $Rb_2Cr_3As_3$ and $Cs_2Cr_3As_3$[32,33] suggests that the electron-mass renormalization factor decreases significantly with the interchain distance. Furthermore, there is a positive correlation between T_c and the Sommerfeld coefficient γ_N (Fig. 2). What controls the electron correlations? How do the electron correlations determine T_c as well as the superconducting pairing? What is the role of one dimensionality on superconductivity? These questions remains open at present.

Remarkably, the Cr-based Q1D arsenides show evidence of unconventional superconductivity with a possible spin-triplet pairing. Theoretical investigations based on an effective theoretical model[38–41] show that the most attractive pairing interactions are always in spin-triplet channels. Spin-triplet superconductivity is also suggested by the theoretical analyses in terms of the multiband TLL scenario[31,36] and melting of macroscopic spin polarization in a weakly coupled odd-gon-unit system.[42] Nevertheless, spin-singlet pairing with a d_{z^2}-

like gap function is obtained from a phenomenological two-band model.[37] Note that conventional electron-phonon mediated superconductivity is also proposed for $K_2Cr_3As_3$.[43] The calculated total electron-phonon coupling constant is as large as $\lambda_{ep} = 3.0$, which seems too high to maintain the lattice.

Experimentally, the ^{75}As Knight shift data[44] indicate the existence of ferromagnetic spin fluctuations, in favor of spin-triplet pairing, consistent with the theoretical calculations and analyses.[30,32] Additionally, the zero-field μSR measurements show evidence of the spontaneous appearance of an internal magnetic field below T_c.[45] The NMR investigations show no Hebel–Slichter coherence peak,[35,44,46] against conventional superconductivity. Furthermore, the Cr-spin fluctuations are captured from the nuclear spin-lattice relaxation rate $1/T_1$, implying non-phonon-mediated superconductivity. It was found that, with increasing the interchain distance, the strength of Cr spin fluctuations is progressively suppressed, together with the decrease in T_c.[46] The inelastic neutron scattering in $K_2Cr_3As_3$ also indicates the existence of short-range magnetic fluctuations, which suggests proximity to a magnetic instability.[47] The incipient magnetic order is considered to couple strongly to the lattice and competes with superconductivity as well. As for the properties of the superconducting gap function, most experiments (including NMR,[35] μSR,[45,48] penetration depth,[49,50] and specific heat[51]) mostly suggest the existence of line nodes, again favoring unconventional superconductivity.

The upper critical field (H_{c2}) of $A_2Cr_3As_3$ appears to be very unusual,[14] which also gives valuable information on the superconducting pairing. Nevertheless, there were very different interpretations to the experimental data.[17,52–54] To clarify the related issues clearly, in this paper, we present some basic knowledge first, then focus on the details of temperature and angular dependence of H_{c2}, and finally try to discuss the result on an equal footing.

3. $H_{c2}(T)$ versus pair breaking

To understand the electron pairing in a superconductor, an alternative method is to investigate how the pairs are broken. The upper critical magnetic field H_{c2} of a type-II superconductor may serve as an indicator for unconventional superconductivity.[3] In the following, we first address how Cooper pairs are broken in a type-II superconductor if an external magnetic field is applied. Then, we present the general experimental method for the measurements of H_{c2}. We will focus on the H_{c2} data as functions of temperature and field direction in the $A_2Cr_3As_3$ superconductors. The implication on the possible superconducting pairing symmetry is discussed. Note that this article has some overlap with our recent publications.[14,53,54]

As is known, superconductors can be classified into type-I and type-II superconductors, according to their responses to external magnetic fields. Unlike type-I superconductors, which show full diamagnetism (Meissner effect) until the external field exceeds the thermodynamic critical field H_c, type-II superconductors are characterized by an additional phase, the mixed state (or vortex state), which contains quantized magnetic fluxons. The two phase boundaries (Meissner to mixed state and mixed state to normal state) define lower and upper critical fields, namely, H_{c1} and H_{c2}. According to Ginzburg–Landau (GL) theory, the borderline of type-I and type-II superconductors locates at $\kappa = \lambda/\xi = 1/\sqrt{2}$, where κ is the so-called GL parameter, λ and ξ denote magnetic penetration depth and superconducting coherence length, respectively. In the case of orbital pair breaking, H_{c2} relates to ξ by the formula $H_{c2}^{\parallel} = \Phi_0/(2\pi\xi_{\perp}^2)$.

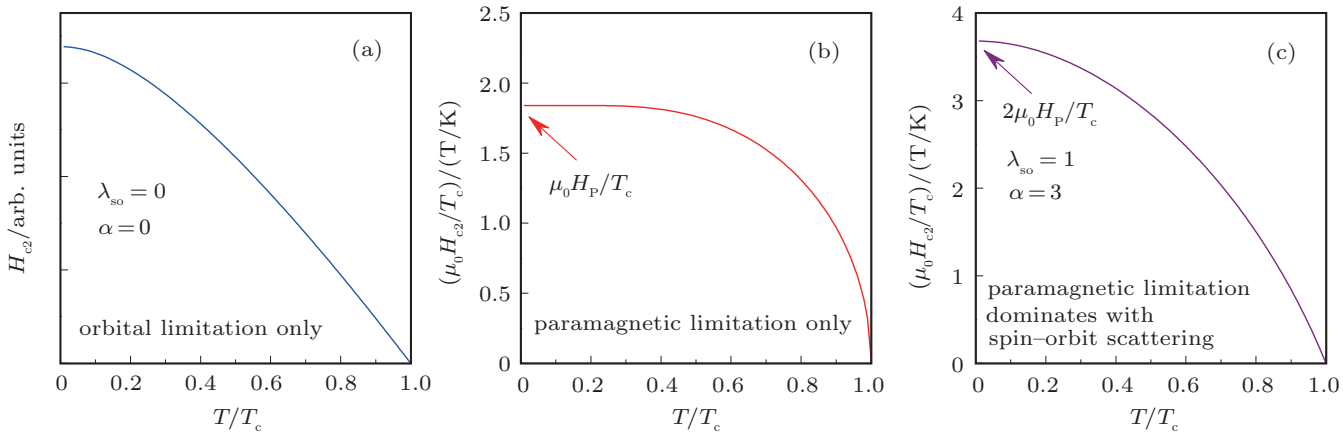


Fig. 4. (color online) Simulations of temperature dependence of upper critical field with different pair-breaking mechanisms. Panel (a) represents the scenario of purely orbital limitation. Panel (b) describes the purely paramagnetic-limited case without spin–orbit scattering. Panel (c) gives an example in which both mechanisms take effect and, the spin–orbit scattering effect is included. The results in panels (a) and (c) are based on Werthammer–Helfand–Hohenberg theory.[55] λ_{so} denotes the strength of spin–orbit scattering. The Maki parameter[56] α is defined by $\sqrt{2}H_{c2}^{orb}(0)/H_P$, where $H_{c2}^{orb}(0)$ is the purely orbitally limited value at zero temperature, H_P denotes the Pauli-paramagnetic limit.

In general, a magnetic field suppresses superconductivity through the following two mechanisms. The first is the orbital pair breaking due to electromagnetic interactions, which is described by GL equations.[57] The purely orbital pair breaking limits the $H_{c2}(T)$ in a way characterized by a linear relation at $T \to T_c$, as shown in Fig. 4(a). The second is the so-called paramagnetic effect,[58,59] which is due to the difference in spin susceptibility between superconducting and normal states (the spin susceptibility of a spin-singlet superconductor is zero). If there were no orbital effects, then the spin paramagnetic effect by itself would yield $H_{c2} = \Delta/(\sqrt{2}\mu_B)$ (here the electron g factor is given to be 2.0), where Δ is the superconducting energy gap. Given the BCS result with $\Delta_0 = 1.76T_c$, one obtains the so-called Pauli-paramagnetic (or Clogston–Chandrasekhar) limit, $\mu_0 H_P(0) = 1.84T_c$ (in unit Tesla).[58,59] Note that paramagnetic pair breaking is featured by a concave-down curvature, as shown in Fig. 2(b), and $H_{c2}(T)^{\text{Pauli}} \propto \sqrt{1-T/T_c}$ holds near T_c. Since $\sqrt{1-T/T_c}$ grows much faster than $(1-T/T_c)$ with decreasing T, therefore, an orbital pair breaking mostly dominates at $T \to T_c$.

The Pauli-paramagnetic limit can be exceeded either by strong coupling or by spin–orbit scattering. The latter effect can be parameterized by the Werthammer–Helfand–Hohenberg (WHH) theory,[55] which simultaneously includes both pair-breaking effects together with spin–orbit scattering [Fig. 4(c)]. It is found that spin–orbit scattering counteracts the paramagnetic effect in limiting H_{c2}. As a result, the H_{c2} can be significantly enhanced through spin–orbit scattering. Note that, in certain circumstances, a novel Fulde–Ferrel–Larkin–Ovchinnikov (FFLO) state with spatial modulations of superconducting order parameter may appear at high fields. The appearance of FFLO often accompanies an upturn in $H_{c2}(T)$.[60,61]

In fact, the pair-breaking effect displayed in Fig. 4 only applies for simple isotropic, s-wave gap, and single-band cases, without the considerations of strong coupling, electron-mass anisotropy, nodal gap, and multiband scenarios. In particular, if the Cooper pairs are in a spin-triplet configuration, which can also be spin-polarized by the external field, then no paramagnetic effect is expected at certain field directions. In a spin-triplet pairing, the superconducting order parameter is expressed using a so-called $\boldsymbol{d}$ vector,[1] thus only a certain field direction may avoid the paramagnetic pair breaking. In contrast, orbital pair breaking by electromagnetic interactions always exists (with exceptions for an extremely large anisotropy) regardless of the spin structure of the superconducting Cooper pairs. We will come back to this point later.

4. Measurement of H_{c2}

In general, H_{c2} is measured by the sharp superconducting transition in a physical quantity under external magnetic fields. The physical quantities can be resistivity, ac susceptibility, dc magnetization, and heat capacity, etc. Two experimental modes can be employed, namely, field-sweep at a fixed temperature and temperature-sweep at a fixed field, which give $H_{c2}(T)$ and $T_c(H)$, respectively. One should find a suitable technique for the H_{c2} measurement, compatible with the specific cases and experimental conditions.

Among the different techniques mentioned above, measurement of resistivity under magnetic fields is the most common one, since it is relatively easily operated and accessible. Figure 5 shows an example for the anisotropic $H_{c2}(T)$ measurement of $Rb_2Cr_3As_3$ crystals. Note that different crystals had to be used for different field directions owing to the sample's extreme sensitivity to moisture (tiny moisture may deteriorate the sample) and also the apparatus' incapability to rotate the sample *in situ*. What we emphasize here is about the criterion of $T_c(H)$ in T-sweep (or $H_{c2}(T)$ in H-sweep). H_{c2} can be regarded as the lowest field in which the first magnetic vortex is allowed to enter the sample's interior. Therefore, the junction between superconducting and normal states should be the position of $T_c(H)$ (or $H_{c2}(T)$), if superconducting thermal fluctuations are not remarkable. That is why here we employ onset superconducting temperature for the determination of $T_c(H)$.

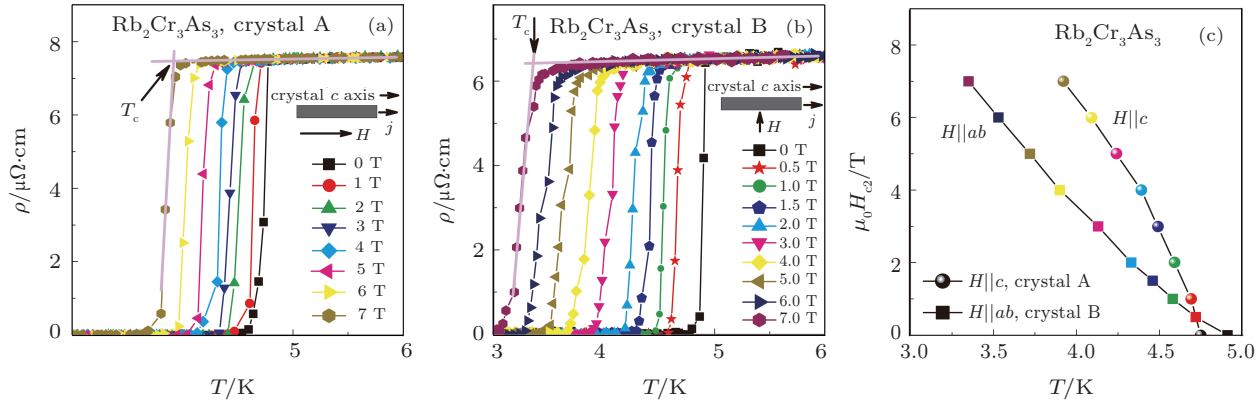


Fig. 5. (color online) Measurement of anisotropic upper critical fields exemplified by temperature dependence of resistivity for $Rb_2Cr_3As_3$ crystals under magnetic fields along (a) and perpendicular to (b) the crystallographic c axis. The resulting $T_c(H)$ data are plotted in panel (c), yielding the superconducting phase diagrams (from Ref. [54]). The crossing between 4.5 K and 5 K comes from different samples (with slightly different T_c values) employed.

In this work we employed a pulsed magnetic field up to 60 T in Wuhan's National High Magnetic Field Center for the H_{c2} measurement of $K_2Cr_3As_3$ crystals. For the high-field measurement of $Rb_2Cr_3As_3$, we also employed the Cell 1 Water-Cooling Magnet of the High Magnetic Field Laboratory of the Chinese Academy of Sciences, which generates the maximum magnetic field up to 38.5 T and allows the magnetoresistance measurement down to 0.3 K. Note that it is very important to avoid the sample's deterioration and keep the electrodes on the sample effective during the measurement.

5. Temperature dependence of H_{c2}

5.1. $K_2Cr_3As_3$ and $Na_2Cr_3As_3$

Figure 6 shows the magneto-resistivity measurement result for $K_2Cr_3As_3$ polycrystals, which gives an initial $H_{c2}(T)$ slope of $\mu_0(\mathrm{d}H_{c2}/\mathrm{d}T)|_{T_c} = \mu_0 H'_{c2} = -7.43$ T/K.[10] By using the WHH formula without spin–orbit coupling,[55] one obtains a zero-temperature upper critical field of $\mu_0 H_{c2}(0) \approx 32$ T, which is three times the Pauli-paramagnetic limit $\mu_0 H_P = 1.84 T_c = 11$ T. Thus the Maki parameter,[56] $\alpha = \sqrt{2} H_{c2}^{orb}(0)/H_P$, is above 4, suggesting either a dominant Pauli-limiting effect at low temperatures or a novel spin-triplet superconductivity. In the case of $Na_2Cr_3As_3$, the $\mu_0 H_{c2}(0)$ value is estimated to be 54 T,[16] 3.4 times of its Pauli limit (16 T). The result contrasts with another Q1D superconductor $Tl_2Mo_6Se_6$ with $T_c = 4.2$ K, whose $\mu_0 H_{c2}(0)$ values are merely 5.8 T and 0.47 T, respectively, for magnetic fields parallel and perpendicular to the c axis.[62] Nevertheless, a large $H_{c2}(0)$ beyond the Pauli limit is seen in Q1D $Li_{0.9}Mo_6O_{17}$,[63] which is regarded as evidence of spin-triplet superconductivity.[64]

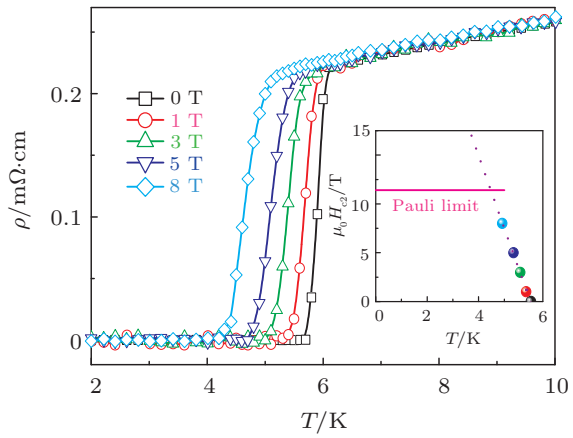


Fig. 6. (color online) The preliminary $H_{c2}(T)$ measurement for $K_2Cr_3As_3$ polycrystals, giving an initial $H_{c2}(T)$ slope of -7.43 T/K. The Pauli limit is marked with the horizontal line in the inset (adapted from Ref. [10]).

Recalling that T_c decreases monotonically with applying pressures, very interestingly, the $\mu_0 H_{c2}(T)$ of the pressurized sample of $K_2Cr_3As_3$ decreases much faster than T_c itself.[19] The $\mu_0 H_{c2}(0)$ value decreases to below the Pauli limit at above 2 GPa. The estimated Maki parameter drops from 4 at ambient pressure to well below 1 at $P > 2$ GPa, indicating a crossover from Pauli-paramagnetic limitation to orbital limitation. If the high $\mu_0 H_{c2}(0)$ value at ambient pressure represents a sign of spin-triplet pairing, the pressure-induced suppression of $\mu_0 H_{c2}(0)$ may suggest a breakdown of the spin-triplet pairing channel upon applying pressures.

Kong, Bud'ko, and Canfield[17] first reported the anisotropic H_{c2} in $K_2Cr_3As_3$ crystals. The initial $H_{c2}(T)$ slopes were measured to be -7 T/K and -12 T/K, respectively, for $\boldsymbol{H} \perp c$ and $\boldsymbol{H} \parallel c$. Meanwhile, the results obtained by Zuo *et al.*[53] are -4.2 T/K and -10.3 T/K, and those by Wang *et al.*[65] are -5 T/K and -16.1 T/K, respectively. Although these data look scattered, primarily because of the sample's sensitivity and the difference in the temperature range of linear fitting, the result points to a relatively weak effective-mass anisotropy with $m_\perp/m_\parallel = (H_{c2}^{\parallel,orb}/H_{c2}^{\perp,orb})^2 =$ 3–10 near T_c. Nevertheless, the upper bound of the effective-mass anisotropy is consistent with the resistivity anisotropy value at $T \to T_c$.[14]

Owing to the expected high H_{c2} at low temperatures, measurements under high magnetic fields are necessary to reveal the whole $H_{c2}(T)$ behavior. Balakirev *et al.*[52] measured $H_{c2}^{\perp}(T)$ and $H_{c2}^{\parallel}(T)$ for $K_2Cr_3As_3$ at high magnetic fields up to 60 T, using a contactless technique based on a proximity detector oscillator. The results show a Pauli-limited behavior for $H_{c2}^{\parallel}(T)$, yet $H_{c2}^{\perp}(T)$ exhibits an orbitally limited behavior with no signs of paramagnetic pair breaking. Consequently, an anomalous reversal in $\gamma_H(T)$ $[= H_{c2}^{\parallel}(T)/H_{c2}^{\perp}(T)]$ appears at ~ 4 K.

We independently conducted the anisotropic H_{c2} measurements for $K_2Cr_3As_3$ crystals by direct magnetoresistance measurement for the first time. A standard four-probe technique was employed, and the sample was installed on a rotator that bears pulsed magnetic fields up to 60 T.[53] Figures 7(a) and 7(b) show the field dependence of the magnetoresistance with $\boldsymbol{H} \perp c$ and $\boldsymbol{H} \parallel c$, respectively. $H_{c2}(T)$ can be clearly identified by the junction points between superconducting and normal states, although no zero-resistance is achieved due to the sample's extreme sensitivity to the environment. The obtained $H_{c2}(T)$ data, plotted in Fig. 7(c), basically agree with those of the previous report.[52] Indeed, $H_{c2}^{\parallel}(T)$ shows a downward curvature, in contrast with the upward curvature for $H_{c2}^{\perp}(T)$. One also sees that $H_{c2}^{\perp}(T)$ and $H_{c2}^{\parallel}(T)$ cross at 3.1 K. The low-temperature H_{c2} values for both field directions exceed the Pauli limit by a factor of 2–3. We will discuss the origin and its implications later on.

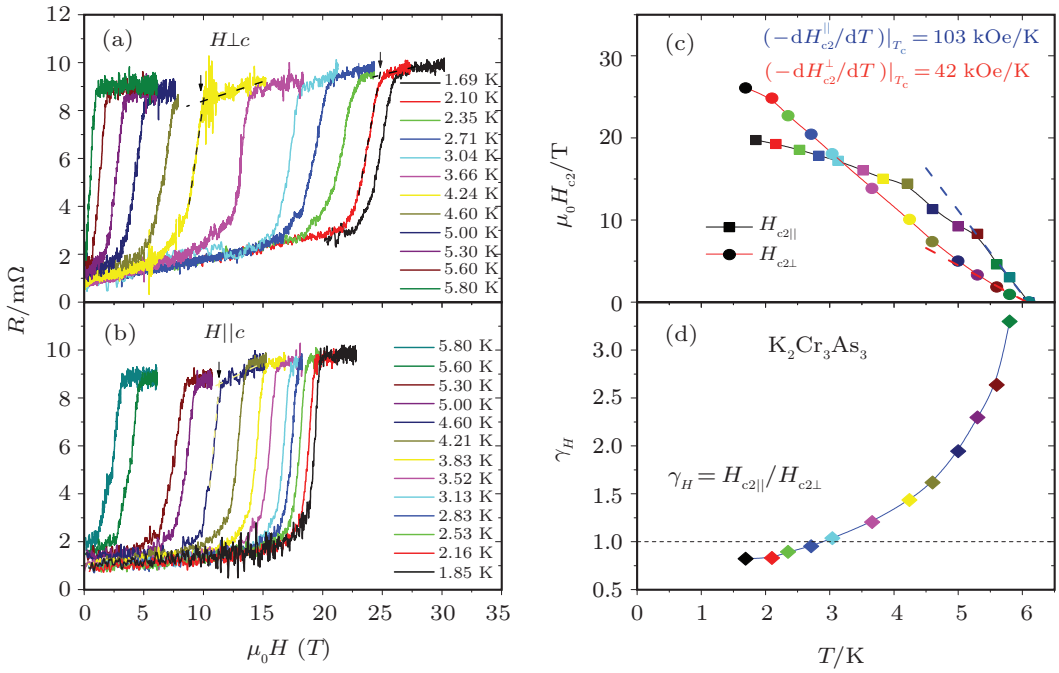


Fig. 7. (color online) Field dependence of resistance at fixed temperatures in $K_2Cr_3As_3$ crystals with the field directions $\boldsymbol{H} \perp c$ (a) and $\boldsymbol{H} \parallel c$ (b). Panels (c) and (d) plot the extracted H_{c2} and the anisotropic parameters $\gamma_H(T) = H_{c2}^{\parallel}/H_{c2}^{\perp}$ as functions of temperature (adapted from Ref. [53]).

5.2. $Rb_2Cr_3As_3$ and $Cs_2Cr_3As_3$

The anisotropic $H_{c2}(T)$ measurement for $Rb_2Cr_3As_3$ under relatively low fields is shown in Fig. 5, from which the $T_c(H)$ data can be directly obtained. As is seen, the superconducting transition moves to lower temperatures with applying magnetic fields, and T_c is suppressed more rapidly for $\boldsymbol{H} \perp c$. The resultant $T_c(H)$ data are plotted in Fig. 5(c). One sees that $H_{c2}^{\parallel}(T)$ exhibits a steeper increase with decreasing temperature, but the magnitude of the slope tends to decrease. By contrast, $H_{c2}^{\perp}(T)$ increases slowly near T_c, yet the magnitude of the slope increases with decreasing temperature. The result in $Cs_2Cr_3As_3$ shown in Fig. 8 is quite similar, although the $H_{c2}(0)$ values are close to the Pauli limit. Therefore, the contrasting $H_{c2}^{\parallel}(T)$ and $H_{c2}^{\perp}(T)$ behavior is universal to all three members of $A_2Cr_3As_3$. As illustrated in Fig. 4, the concave-down feature in $H_{c2}^{\parallel}(T)$ indicates a dominant Pauli-limited pair-breaking mechanism. The almost linear $H_{c2}^{\perp}(T)$ characteristic meets an orbitally limiting mechanism. The slight concave-up behavior may reflect multiband superconductivity since there are three or four FSs in the system.[32,33]

Generally, orbital pair breaking dominates $H_{c2}(T)$ at $T \to T_c$. This means that the initial slope of $H_{c2}(T)$ is a measure of the orbitally-limited upper critical field at zero temperature, $H_{c2}^{\mathrm{orb}}(0)$. From the data in Fig. 5(c), we obtain the initial slopes of $\mu_0 H_{c2}^{\parallel\prime} = -3.0$ T/K and $\mu_0 H_{c2}^{\perp\prime} = -16.7$ T/K, respectively, for $Rb_2Cr_3As_3$. The data of $Cs_2Cr_3As_3$ (in Fig. 8) show $\mu_0 H_{c2}^{\parallel\prime} = -0.9$ T/K and $\mu_0 H_{c2}^{\perp\prime} = -6.3$ T/K. According to GL theory, the effective-mass anisotropy, $m_\perp/m_\parallel = (H_{c2}^{\parallel\prime}/H_{c2}^{\perp\prime})^2$, are about 30 and 50, respectively, for $Rb_2Cr_3As_3$ and $Cs_2Cr_3As_3$. The result suggests stronger Q1D anisotropy in $Rb_2Cr_3As_3$ and $Cs_2Cr_3As_3$, consistent with the larger inter-chain distance in the crystal structure.[14]

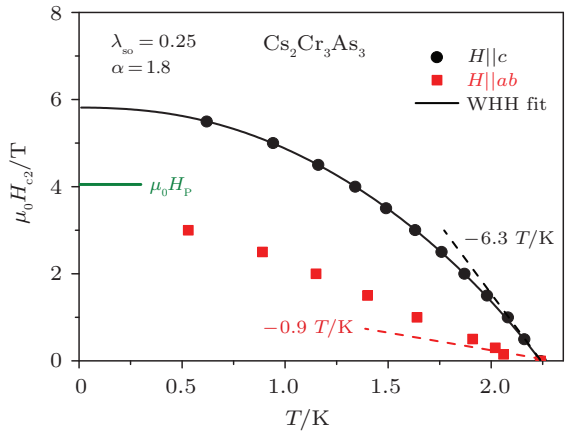


Fig. 8. (color online) Anisotropic $H_{c2}(T)$ versus temperature in $Cs_2Cr_3As_3$ crystals. The solid line is the WHH fitting for $\boldsymbol{H} \parallel c$ (see text for the details).

Figures 9(a) and 9(b) show the field dependence of resistance at fixed temperatures with different field directions in $Rb_2Cr_3As_3$. We employ the identical criterion for the determination of $H_{c2}(T)$. While it is evident to determine the $H_{c2}(T)$ for sample C (with $\boldsymbol{H} \parallel ab$) which shows a single sharp superconducting transition, however, it turns out to be ambiguous for sample D (with $\boldsymbol{H} \parallel c$) because it exhibits two main transitions (possibly arising from the electrode contact problem and/or sample's partial deterioration.[20,21]). Figure 9(c) presents an additional data set for $\boldsymbol{H} \parallel c$, from which we find the steepest transition to use for the $H_{c2}(T)$ determination. The resultant $H_{c2}(T)$ data are displayed in Fig. 9(d). One sees that different sets of data basically meet each other. The H–T phase diagram looks similar to that of $K_2Cr_3As_3$. Firstly,

$H_{c2}^{\parallel}(T)$ shows an obvious downward curvature, characteristic of Pauli-limiting behavior. $H_{c2}^{\parallel}(T)$ tends to saturate to 17.5 T, twice of $\mu_0 H_P$, without any sign of the formation of the FFLO state. The enhanced $H_{c2}^{\parallel}(0)$ seems to be mostly related to the strong coupling superconductivity as evidenced by the large specific-heat jump $[\Delta C/(\gamma T_c) = 2.4]$.[10] Secondly, $H_{c2}^{\perp}(T)$ is approximately linear in the whole temperature range, which strongly suggests the absence of the Pauli-paramagnetic pair breaking effect. In particular, $H_{c2}^{\perp}(T)$ keeps increasing linearly down to $0.075T_c$. This suggests that, apart from the orbitally pair-breaking effect with the typical $H_{c2}(T)$ profile shown in Fig. 4(a), there could be a positive role played by external magnetic fields for superconductivity. Spin-triplet with equal-spin pairing may account for such a novel $H_{c2}(T)$ behavior. Thirdly, the $\gamma_H(T)$ data for $K_2Cr_3As_3$ and $Rb_2Cr_3As_3$ almost coincide with each other, although the latter shows a larger anisotropy close to T_c. In both cases, the apparent γ_H reversal at about $0.4T_c$ actually reflects different pair breaking mechanisms for different field directions. We will further address this issue with the measurement of polar-angle dependence.

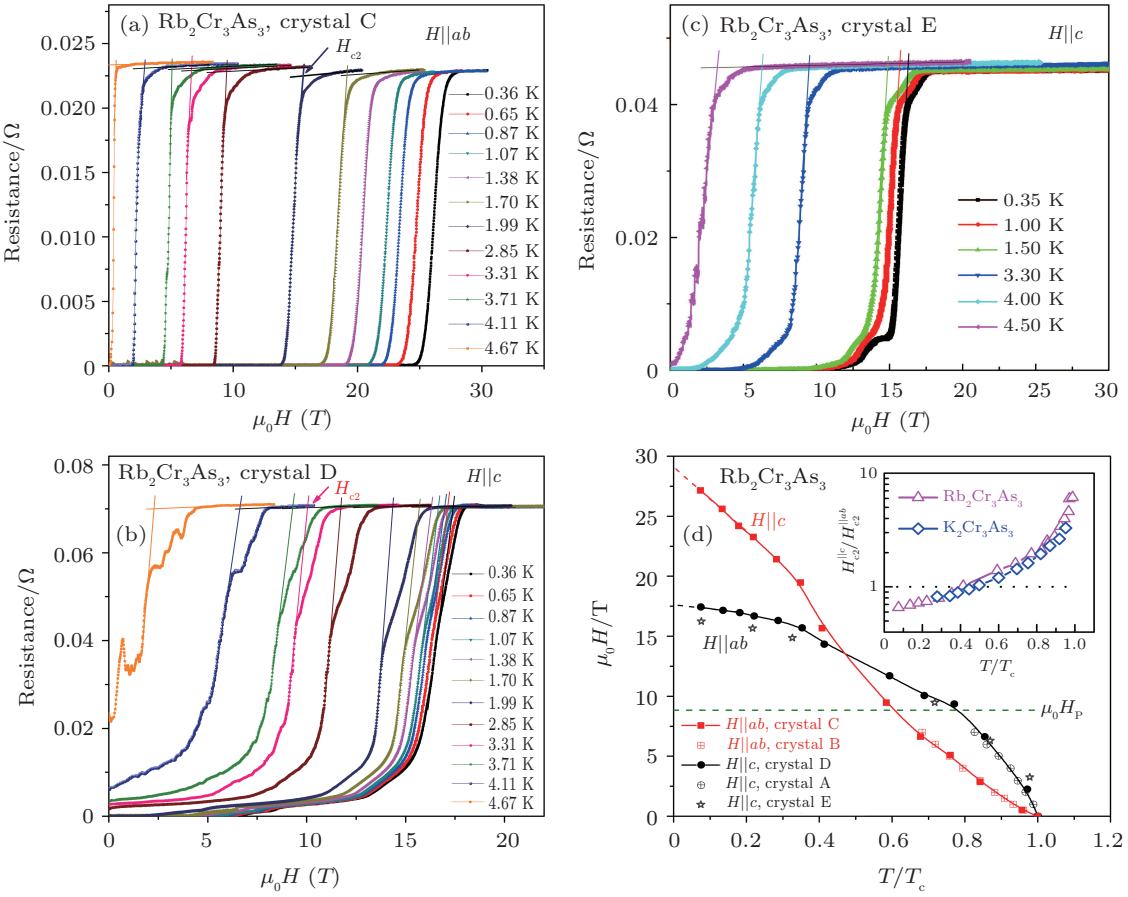


Fig. 9. (color online) (a) and (b) Field dependence of resistance at fixed temperatures below T_c, for $Rb_2Cr_3As_3$ crystals with $\boldsymbol{H} \parallel ab$ and $\boldsymbol{H} \parallel c$, respectively. Panel (c) shows an additional data set for another crystal with $\boldsymbol{H} \parallel c$. Panel (d) summarizes the $H_{c2}(T)$ result in $Rb_2Cr_3As_3$, using T/T_c as the horizontal axis. The Pauli paramagnetic limit is marked. The inset plots the anisotropic parameter $\gamma_H = H_{c2}^{\parallel}/H_{c2}^{\perp}$ in a logarithmic scale (adapted from Ref. [54]).

The phenomenon of γ_H reversal, i.e., crossing between $H_{c2}^{\perp}(T)$ and $H_{c2}^{\parallel}(T)$, has been witnessed in several other systems including the Q1D organic superconductor $(TMTSF)_2PF_6$,[66] iron-based chalcogenides,[61,67,68] and the heavy-fermion superconductor UPt_3.[69] At first sight, the reversal in $\gamma_H(T)$ $K_2Cr_3As_3$ and $Rb_2Cr_3As_3$ suggests a dimension crossover. However, it seems unlikely from the crystal and electronic structure points of view. Moreover, the dimension crossover scenario can be ruled out by our $H_{c2}(\theta)$ data (see below) which show modulations at the "crossover" temperature of 3.1 K. This is definitely inconsistent with the expected angle dependence, $H_{c2}(\theta) \sim (\cos^2\theta + \varepsilon^2 \sin^2\theta)^{-1/2}$, in which a constant H_{c2} is given for the effective-mass ratio $\varepsilon^2 = 1$.

We note that details of the $H_{c2}(T)$ behaviors differ in different systems. In $(TMTSF)_2PF_6$, $H_{c2}(T)$ shows a pronounced upward curvature for the field directions perpendicular to $\boldsymbol{c}^*$ at low temperatures.[66] This arises from the dramatic reduction of the orbitally pair-breaking effect owing to a field-induced dimension crossover.[3] In iron-based superconductors, the $H_{c2}(T)$ data reveal that the Pauli-limiting effect is always at work regardless of the field directions,[61,67] consistent with a spin-singlet pairing. The anisotropy inversion appears only accidentally, and $\gamma_H(T)$ generally approaches 1.0 at $T \to 0$,[70]

which actually reflects the Pauli-paramagnetic pair breaking effect associated with anisotropic spin–orbit coupling. By contrast, the reversed anisotropy ratio in UPt_3 is sizable at zero temperature,[69] similar to the case here in $A_2Cr_3As_3$ (A = K and Rb). As for $Cs_2Cr_3As_3$, although the Maki parameter decreases to 1.8 for $\boldsymbol{H} \parallel c$, the $H_{c2}^{\perp}(T)$ data show a linear dependence, suggesting that there is still a possibility of an absence of the Pauli-limiting effect for $\boldsymbol{H} \parallel ab$.

6. Angle dependence of H_{c2} in $K_2Cr_3As_3$

6.1. Polar-angle dependence

To further clarify if there is any "residual" Pauli-limiting effect for $\boldsymbol{H} \perp c$, we performed the angle dependence measurement. Namely, the sample rotates *in situ* such that the field direction tilts a "polar" angle θ from the c axis, as shown in the inset of Fig. 10. First of all, at temperatures near T_c, $H_{c2}(\theta)$ decreases monotonously with increasing θ (from 0° to 90°). This is understandable since there is a uniaxial effective-mass anisotropy. As the temperature is lowered, an additional maximum in $H_{c2}(\theta)$ appears at $\theta = 90°$. The enhanced H_{c2} is consistent with the reduced Pauli-limiting effect for $\boldsymbol{H} \perp c$.

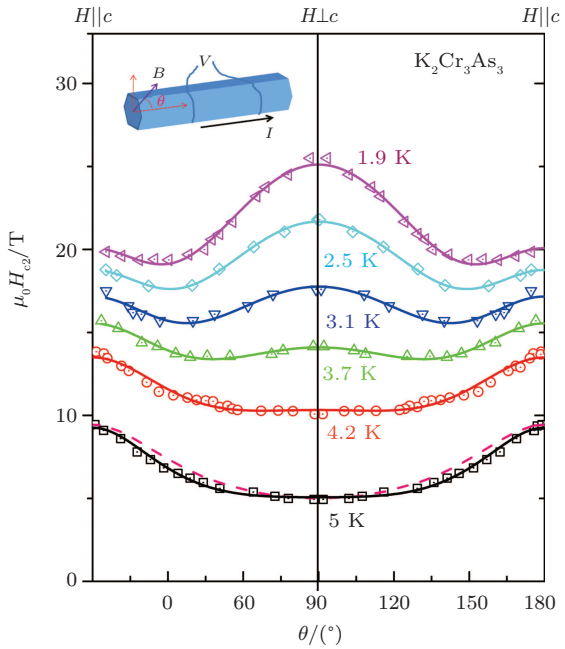


Fig. 10. (color online) Polar angle (θ) dependent $H_{c2}(\theta)$ at fixed temperatures in $K_2Cr_3As_3$. The solid lines are the fitted result using Eq. (2) (see text for details), and the dashed pink curve (for 5-K data only) is the fitted result with Eq. (1) (adapted from Ref. [53]).

Below we show that the whole $H_{c2}(\theta)$ data set can be perfectly explained by the combination of a *fully* anisotropic Pauli-limiting effect (i.e., absence of Pauli-limiting effect for $\boldsymbol{H} \perp c$) with a uniaxial effective-mass anisotropy. According to GL theory, the effective-mass anisotropy leads to the anisotropy of the orbitally limited $H_{c2}^{orb}(\theta)$,

$$H_{c2}^{orb}(\theta) = \frac{H_{c2,\parallel}^{orb}}{\sqrt{\cos^2\theta + \varepsilon^2 \sin^2\theta}}, \quad (1)$$

where $H_{c2,\parallel}^{orb}$ denotes the presumed orbitally limited upper critical field for $\boldsymbol{H} \parallel c$ and, $\varepsilon^2 = m_{\perp}/m_{\parallel} = (H_{c2,\parallel}^{orb}/H_{c2,\perp}^{orb})^2$ is the effective-mass ratio. Indeed, equation (1) can basically describe the experimental $H_{c2}(\theta)$ data at 5 K (albeit of obvious deviations at $\theta = 20°$–$70°$). However, it completely fails to meet the $H_{c2}(\theta)$ data at lower temperatures.

The reason for the failure of Eq. (1) is because the paramagnetic pair breaking effect is not included. Given the contrasting $H_{c2}(T)$ behavior for $\boldsymbol{H} \parallel c$ and $\boldsymbol{H} \perp c$, the paramagnetic pair breaking is assumed to be fully anisotropic. Namely, only the magnetic-field component parallel to the c axis further suppresses the $H_{c2}^{orb}(\theta)$ in Eq. (1). The paramagnetically pair-breaking effect can be parameterized by an effective Pauli-limiting field H_{pm}. Therefore, we have $H_{pm}(\theta) = H_{pm}^{\parallel} \cos\theta$, in which $H_{pm}(\theta) = H_{pm}^{\parallel}$ (fully Pauli limiting) for $\theta = 0°$ and, $H_{pm}(\theta) = 0$ (absence of Pauli limiting) for $\theta = 90°$.

The effective Pauli-limiting field H_{pm} suppresses H_{c2}^{orb} in a way of competition between the related energies.[55,58,59,71] Given $E \sim H^2$, therefore, $[H_{c2}(\theta)]^2 = [H_{c2}^{orb}(\theta)]^2 - [H_{pm}(\theta)]^2$. Consequently, one obtains an explicit expression for $H_{c2}(\theta)$,

$$H_{c2}(\theta) = \sqrt{\frac{(H_{c2,\parallel}^{orb})^2}{\cos^2\theta + \varepsilon^2 \sin^2\theta} - (H_{pm}^{\parallel} \cos\theta)^2}. \quad (2)$$

Remarkably, the whole experimental data set of $H_{c2}(\theta, T)$ satisfies the above equation very well, as shown in Fig. 10, which further clarifies the absence of the Pauli-limiting effect for $\boldsymbol{H} \perp c$. The data fitting yields three parameters, $H_{c2,\parallel}^{orb}$, ε, and $H_{pm}^{\parallel}$ at a given temperature. As expected, the fitted $H_{c2,\parallel}^{orb}(T)$ is basically linear. The linear extrapolation yields a zero-temperature orbitally limited $\mu_0 H_{c2,\parallel}^{orb}(0)$ of 51.5 T for $\boldsymbol{H} \parallel c$, which is reasonably larger than the extrapolated value of $\mu_0 H_{c2,\perp}^{orb}(0) = 37.2$ T for $\boldsymbol{H} \perp c$. The obtained $H_{c2,\parallel}^{orb}(0)$ and $H_{c2,\perp}^{orb}(0)$ exceed the Pauli limit H_{c2}^{P} by a factor of 4.6 and 3.4, respectively. Using the GL relations, $H_{c2,\parallel}^{orb}(0) = \Phi_0/[2\pi\xi_{\perp}(0)^2]$ and $H_{c2,\perp}^{orb}(0) = \Phi_0/[2\pi\xi_{\perp}(0)\xi_{\parallel}(0)]$, where Φ_0 is the flux quantum, the anisotropic coherence lengths at zero temperature can be estimated to be $\xi_{\perp}(0) = 2.53$ nm and $\xi_{\parallel}(0) = 3.50$ nm. The $\xi_{\perp}(0)$ value exceeds twice the interchain distance in $K_2Cr_3As_3$,[10] indicating the nature of anisotropic 3D superconductivity.

6.2. Azimuthal-angle dependence

Figure 11(a) shows derivative of the magnetoresistance for the field directions with different azimuthal ϕ angles. The $H_{c2}(\phi)$ data can be extracted by the peak value in dR/dH (here

we use a different criterion so as to increase the measurement precision). The ϕ angle varied from 1.87° to 153.38°. According to the crystal symmetry with the point group of D_{3h}, the data set is rotated by 120° and −120°, respectively, in order to plot a complete polar diagram. One sees that the overlapped region matches well, which validates the rotation. Consequently, the obtained $H_{c2}(\phi)$ profile shows a three-fold modulation with an amplitude of 0.36 T. The maximum of $H_{c2}(\phi)$ appears for the field directions along the crystallographic a and b axes. Here the possibility of surface superconductivity and the influence of anisotropic normal-state magnetoresistance can be excluded (see the Supplementary Materials in Ref. [53]). Note that the $H_{c2}(\phi)$ modulation (with a relative magnitude up to ∼ 1.2%) in $K_2Cr_3As_3$ is actually more obvious than those in UPt_3[72] and MgB_2,[73] both of which also crystallize in a hexagonal lattice.

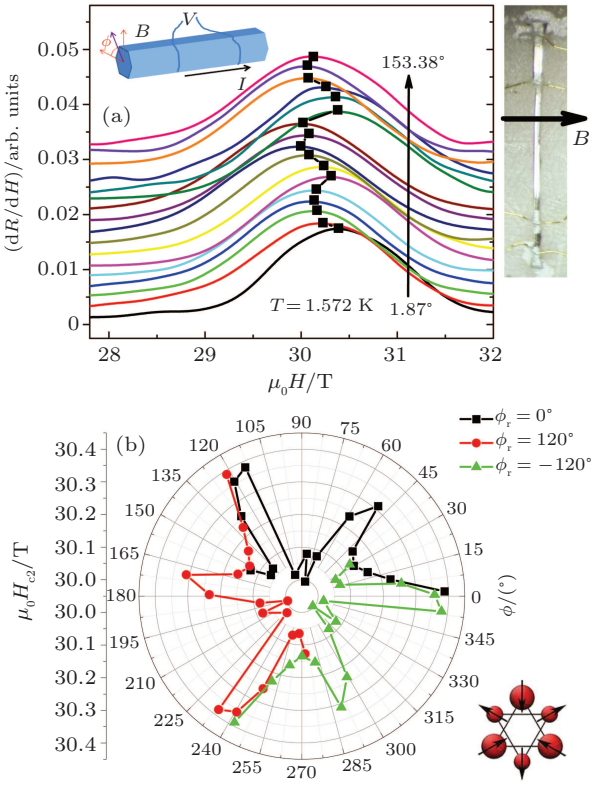


Fig. 11. (color online) In-plane azimuthal-angle dependence $H_{c2}(\phi)$ at 1.572 ± 0.001 K for $K_2Cr_3As_3$. (a) The derivatives of $R(H)$ for different ϕ angles, from which H_{c2} is obtained. (b) Polar plot of the extracted $H_{c2}(\phi)$. The red (blue) triangles come from the rotation of the derived data with $\phi_r = 120°$ (−120°), respectively. Shown at the upper right is the photograph of the sample configuration in the measurement. The lower-right corner shows the possible Cr_6-octahedron spin order for the magnetic ground state, according to first-principles calculations (adapted from Ref. [53]).

The sixfold modulation of $H_{c2}(\phi)$ in UPt_3[72] can be explained in terms of a coupling to the symmetry breaking field.[74] In the case of $K_2Cr_3As_3$, according to the first-principles calculations, the magnetic ground state appears to be a novel in-out co-planar magnetic order,[30,32] as shown at the lower-right corner in Fig. 11(b). The magnetic moments lie in the basal plane. Intuitively, this result seems to be compatible with the observed $H_{c2}(\phi)$ modulation that can be similarly explained by the coupling to the symmetry breaking field.

7. Discussion and conclusion

For a conventional superconductor with a high $H_{c2}(0)$ comparable to H_P, the $H_{c2}(0)$ value is normally limited by the paramagnetic effect regardless of field directions. Considering the paramagnetically limited behavior of $H_{c2}^{\parallel}(T)$ in $K_2Cr_3As_3$, as well as the preliminary observation of the insensitivity of T_c on impurity scattering, Balakirev *et al.*[52] proposed a novel spin-singlet superconductivity. The absence of the Pauli-limiting effect for $\boldsymbol{H} \perp c$ is explained by assuming electron-spin locking along the c direction. In fact, we have demonstrated that the apparent insensitivity of T_c on impurity scattering is due to the clean limit ($l \gg \xi$) for the superconductivity (see below). So, their staring point seems to have deviated. Secondly, according to the first-principles calculations,[30,32] the Cr moments likely align perpendicular to the chain direction that is possibly associated with the sizable spin–orbit coupling shown in Fig. 3(c), contradicting with the Ising-like spin-locking scenario. More importantly, our in-plane $H_{c2}(\phi)$ profile also opposes the Ising-like spin-singlet superconductivity.

We argue that spin-triplet pairing explains the overall H_{c2} data more naturally. The absence of the Pauli-limiting effect for $H_{c2}^{\perp}(T)$ and a large $H_{c2}^{\perp}(0)$ value (3.4 times of H_P) actually dictate a spin-triplet pairing scenario, as in the case of UPt_3.[4] The latter was recently confirmed to host a spin-triplet odd-parity superconductivity.[75] The (pseudo)spins of the odd-parity Cooper pairs are $|\uparrow\downarrow\rangle + |\downarrow\uparrow\rangle$ with $S_z = 0$, which is equivalent to the spin state of $|\leftleftarrows\rangle + |\rightrightarrows\rangle$. In this circumstance, the Zeeman energy breaks the Cooper pairs for $\boldsymbol{H} \| c$, hence the Pauli-limiting behavior for $H_{c2}^{\parallel}(T)$. By contrast, the perpendicular field simply changes the population of Cooper pairs with spin directions $|\leftleftarrows\rangle$ and $|\rightrightarrows\rangle$, and therefore, no paramagnetic pair-breaking is expected for $H_{c2}^{\perp}(T)$. Indeed, by taking spin-triplet pairing into consideration, and with some simplifications and approximations, we are able to derive an equation for $H_{c2}(\theta)$, whose solution is consistent with Eq. (2) (for details see the Supplementary Materials in Ref. [53]). Here we note that, owing to the non-centrosymmetric crystal structure in $K_2Cr_3As_3$, the pairing symmetry is in principle a mixture of singlet and triplet states,[38] except for the case of a simple p_z wave in which a purely triplet pairing is anticipated because of the mirror-plane reflection symmetry.[39]

Finally, we comment on the impurity scattering effect on T_c, which is important to judge the possibility of either the singlet or triplet pairing state. For an odd-parity unconventional

superconductor, nonmagnetic scattering serves as a source of pair breaking even at zero field, hence T_c suppression is expected. However, such an impurity scattering effect will not be evident in the clean-limit regime, i.e., the electron mean free path l is much larger than the superconducting coherence length ξ. In $K_2Cr_3As_3$, l is estimated to be ~ 75 nm (after the electron-mass renormalization is considered) for the electron transport along the c axis in the sample with RRR = 61, and $\xi_{\|}(0)$ is only 3.5 nm, thus $l \gg \xi$ holds. A similar case is seen in $Rb_2Cr_3As_3$.[54] This explains why the T_c keeps almost unchanged for single-crystal samples with different RRRs. Our recent study shows that, when introducing sufficient impurities ($l \sim \xi$), T_c is indeed suppressed in $K_2Cr_3As_3$.[15]

In conclusion, we show that the detailed H_{c2} measurements supply very important information on the superconducting pairing of the Q1D Cr-based superconductors. The apparent "anisotropy-reversal" phenomenon actually reflects different pair-breaking mechanisms for different magnetic-field directions. The absence of paramagnetic pair breaking for $\boldsymbol{H} \perp c$ is further clarified by the $H_{c2}(\theta)$ data set in $K_2Cr_3As_3$. The three-fold modulation in $H_{c2}(\phi)$ implies time-reversal symmetry breaking in the superconducting state. The spin structure of the superconducting Cooper pairs probably involves Cr-spin locking within the ab plane, and the dominant pairing is likely to be of a spin-triplet state, which seems more natural to explain the full $H_{c2}(\theta, \phi, T)$ data. So far, the spin-triplet pairing scenario is consistent with the previous suggestions in experimental and theoretical investigations. Nevertheless, clarification of the specific pairing symmetry needs more investigations.

Unconventional superconductivity has been and remains one of the major topics in the area of condensed matter physics. According to the classification by Hirsch, Maple, and Marsiglio,[76] there are 11 classes of materials that can be categorized into "unconventional superconductors" in which superconductivity does not come from conventional electron-phonon interactions. The present status of the research, in particular, with the H_{c2} measurement, strongly suggests that the newly discovered $A_2Cr_3As_3$ superconductors should belong to the unconventional category.

Acknowledgment

We thank Pi L, Xi C Y, Bao J K, Tang Z T, Liu Y, Zuo H K, Wang J H, Kang J, Xu Z A, Yuan H Q, Cao C, Ning F L, Imai T, Zheng G Q, and Sun L L for our fruitful collaborations. Thanks are also due to Agterberg D F, Zhang F C, Zhou Y, Dai J H, Luo J L, Cheng J G, Yang F, and Hu J P for their helpful discussions.

References

[1] Sigrist M and Ueda K 1991 *Rev. Mod. Phys.* **63** 239
[2] Jerome D 1991 *Science* **252** 1509
[3] Zhang W and De Melo C A R S 2007 *Adv. Phys.* **56** 545
[4] Sauls J A 1994 *Adv. Phys.* **43** 113
[5] Joynt R and Taillefer L 2002 *Rev. Mod. Phys.* **74** 235
[6] Mackenzie A P and Maeno Y 2003 *Rev. Mod. Phys.* **75** 657
[7] Huxley A D 2015 *Physica C* **514** 368
[8] Wu W, Cheng J, Matsubayashi K, Kong P, Lin F, Jin C, Wang N, Uwatoko Y and Luo J 2014 *Nat. Commun.* **5** 5508
[9] Cheng J G 2017 *Acta Phys. Sin.* **66** 037401
[10] Bao J K, Liu J Y, Ma C W, Meng Z H, Tang Z T, Sun Y L, Zhai H F, Jiang H, Bai H, Feng C M, Xu Z A and Cao G H 2015 *Phys. Rev. X* **5** 011013
[11] Tang Z T, Bao J K, Liu Y, Sun Y L, Ablimit A, Zhai H F, Jiang H, Feng C M, Xu Z A and Cao G H 2015 *Phys. Rev. B* **91** 020506
[12] Tang Z T, Bao J K, Wang Z, Bai H, Jiang H, Liu Y, Zhai H F, Feng C M, Xu Z A and Cao G H 2015 *Sci. China-Materials* **58** 16
[13] Hu J 2015 *Sci. Bull.* **60** 2140
[14] Cao G H, Bao J K, Tang Z T, Liu Y and Jiang H 2017 *Phil. Mag.* **97** 591
[15] Liu Y, Bao J K, Zuo H K, Ablimit A, Tang Z T, Feng C M, Zhu Z W and Cao G H 2016 *Sci. China-Phys. Mech. Astron.* **59** 657402
[16] Mu Q G, Ruan B B, Pan B J, Liu T, Yu J, Zhao K, Chen G F and Ren Z A 2018 *Phys. Rev. Mater.* **2** 034803
[17] Kong T, Budko S L and Canfield P C 2015 *Phys. Rev. B* **91** 020507
[18] Wang Z, Yi W, Wu Q, Sidorov V A, Bao J, Tang Z, Guo J, Zhou Y, Zhang S, Li H, Shi Y, Wu X, Zhang L, Yang K, Li A, Cao G, Hu J, Sun L and Zhao Z 2016 *Sci. Rep.* **6** 37878
[19] Sun J P, Jiao Y Y, Yang C L, Wu W, Yi C J, Wang B S, Shi Y G, Luo J L, Uwatoko Y and Cheng J G 2017 *J. Phys.: Condens. Matter* **29** 455603
[20] Bao J K, Li L, Tang Z T, Liu Y, Li Y K, Bai H, Feng C M, Xu Z A and Cao G H 2015 *Phys. Rev. B* **91** 180404
[21] Tang Z T, Bao J K, Liu Y, Bai H, Jiang H, Zhai H F, Feng C M, Xu Z A and Cao G H 2015 *Sci. China-Materials* **58** 543
[22] Mu Q G, Ruan B B, Pan B J, Liu T, Yu J, Zhao K, Chen G F and Ren Z A 2017 *Phys. Rev. B* **96** 140504
[23] Liu T, Mu Q G, Pan B J, Yu J, Ruan B B, Zhao K, Chen G F and Ren Z A 2017 *Europhys. Lett.* **120** 27006
[24] Jiang H, Bao J K, Zhai H F, Tang Z T, Sun Y L, Liu Y, Wang Z C, Bai H, Xu Z A and Cao G H 2015 *Phys. Rev. B* **92** 205107
[25] Ablimit A, Sun Y L, Jiang H, Bao J K, Zhai H F, Tang Z T, Liu Y, Wang Z C, Feng C M and Cao G H 2017 *J. Alloys Compd.* **694** 1149
[26] Wang W S, Gao M, Yang Y, Xiang Y Y and Wang Q H 2017 *Phys. Rev. B* **95** 144507
[27] Edelmann M, Sangiovanni G, Capone M and de Medici L 2017 *Phys. Rev. B* **95** 205118
[28] Moser J, Gabay M, Auban-Senzier P, Jérome D, Bechgaard K and Fabre J 1998 *Eur. Phys. J. B* **1** 39
[29] Biermann S, Georges A, Lichtenstein A and Giamarchi T 2001 *Phys. Rev. Lett.* **87** 276405
[30] Jiang H, Cao G and Cao C 2015 *Sci. Rep.* **5** 16054
[31] Zhong H, Feng X Y, Chen H and Dai J 2015 *Phys. Rev. Lett.* **115** 227001
[32] Wu X X, Le C C, Yuan J, Fan H and Hu J P 2015 *Chin. Phys. Lett.* **32** 057401
[33] Alemany P and Canadell E 2015 *Inorg. Chem.* **54** 8029
[34] Watson M D, Feng Y, Nicholson C W, Monney C, Riley J M, Iwasawa H, Refson K, Sacksteder V, Adroja D T, Zhao J and Hoesch M 2017 *Phys. Rev. Lett.* **118** 097002
[35] Zhi H Z, Imai T, Ning F L, Bao J K and Cao G H 2015 *Phys. Rev. Lett.* **114** 147004
[36] Miao J J, Zhang F C and Zhou Y 2016 *Phys. Rev. B* **94** 205129
[37] Wachtel G and Kim Y B 2016 *Phys. Rev. B* **94** 104522
[38] Zhou Y, Cao C and Zhang F C 2017 *Sci. Bull.* **62** 208
[39] Wu X, Yang F, Le C, Fan H and Hu J 2015 *Phys. Rev. B* **92** 104511
[40] Zhang L D, Wu X, Fan H, Yang F and Hu J 2016 *Europhys. Lett.* **113** 37003
[41] Cao G H 2017 *Sci. Bull.* **62** 206
[42] Reja S and Nishimoto S 2018 arXiv: 1801.06204
[43] Subedi A 2015 *Phys. Rev. B* **92** 174501

[44] Yang J, Tang Z T, Cao G H and Zheng G Q 2015 *Phys. Rev. Lett.* **115** 147002

[45] Adroja D T, Bhattacharyya A, Telling M, Feng Y, Smidman M, Pan B, Zhao J, Hillier A D, Pratt F L and Strydom A M 2015 *Phys. Rev. B* **92** 134505

[46] Zhi H, Lee D, Imai T, Tang Z, Liu Y and Cao G 2016 *Phys. Rev. B* **93** 174508

[47] Taddei K M, Zheng Q, Sefat A S and de la Cruz C 2017 *Phys. Rev. B* **96** 180506

[48] Adroja D, Bhattacharyya A, Smidman M, Hillier A, Feng Y, Pan B, Zhao J, Lees M R, Strydom A and Biswas P K 2017 *J. Phys. Soc. Jpn.* **86** 044710

[49] Pang G M, Smidman M, Jiang W B, Bao J K, Weng Z F, Wang Y F, Jiao L, Zhang J L, Cao G H and Yuan H Q 2015 *Phys. Rev. B* **91** 220502

[50] Pang G M, Smidman M, Jiang W B, Shi Y G, Bao J K, Tang Z T, Weng Z F, Wang Y F, Jiao L, Zhang J L, Luo J L, Cao G H and Yuan H Q 2016 *J. Magn. Magn. Mater.* **400** 84

[51] Shao Y T, Wu X X, Wang L, Shi Y G, Hu J P and Luo J L 2018 *Phys. Rev. B*, submitted

[52] Balakirev F F, Kong T, Jaime M, McDonald R D, Mielke C H, Gurevich A, Canfield P C and Budko S L 2015 *Phys. Rev. B* **91** 220505

[53] Zuo H, Bao J K, Liu Y, Wang J, Jin Z, Xia Z, Li L, Xu Z, Kang J, Zhu Z and Cao G H 2017 *Phys. Rev. B* **95** 014502

[54] Tang Z T, Liu Y, Bao J K, Xi C Y, Pi L and Cao G H 2017 *J. Phys.: Condens. Matter* **29** 424002

[55] Werthamer N R, Helfand E and Hohenberg P C 1966 *Phys. Rev.* **147** 295

[56] Maki K 1966 *Phys. Rev.* **148** 362

[57] Helfand E and Werthamer N R 1966 *Phys. Rev.* **147** 288

[58] Clogston A M 1962 *Phys. Rev. Lett.* **9** 266

[59] Chandrasekhar B S 1962 *Appl. Phys. Lett.* **1** 7

[60] Gurevich A 2010 *Phys. Rev. B* **82** 184504

[61] Gurevich A 2011 *Rep. Prog. Phys.* **74** 124501

[62] Petrović A P, Lortz R, Santi G, Decroux M, Monnard H, Fischer O, Boeri L, Andersen O K, Kortus J, Salloum D, Gougeon P and Potel M 2010 *Phys. Rev. B* **82** 235128

[63] Mercure J F, Bangura A F, Xu X, Wakeham N, Carrington A, Walmsley P, Greenblatt M and Hussey N E 2012 *Phys. Rev. Lett.* **108** 187003

[64] Sepper O and Lebed A G 2014 *Phys. Rev. B* **90** 094509

[65] Wang X F, Roncaioli C, Eckberg C, Kim H, Yong J, Nakajima Y, Saha S R, Zavalij P Y and Paglione J 2015 *Phys. Rev. B* **92** 020508

[66] Lee I J, Naughton M J, Danner G M and Chaikin P M 1997 *Phys. Rev. Lett.* **78** 3555

[67] Khim S, Kim J W, Choi E S, Bang Y, Nohara M, Takagi H and Kim K H 2010 *Phys. Rev. B* **81** 184511

[68] Maiorov B, Mele P, Baily S A, Weigand M, Lin S Z, Balakirev F F, Matsumoto K, Nagayoshi H, Fujita S, Yoshida Y, Ichino Y, Kiss T, Ichinose A, Mukaida M and Civale L 2014 *Supercond. Sci. Technol.* **27** 044005

[69] Shivaram B S, Rosenbaum T F and Hinks D G 1986 *Phys. Rev. Lett.* **57** 1259

[70] Yuan H Q, Singleton J, Balakirev F F, Baily S A, Chen G F, Luo J L and Wang N L 2009 *Nature* **457** 565

[71] Hake R R 1967 *Appl. Phys. Lett.* **10** 189

[72] Keller N, Tholence J L, Huxley A and Flouquet J 1994 *Phys. Rev. Lett.* **73** 2364

[73] Tamegai T, Shi Z, Pradhan A K, Nakamura H, Ghosh A K, Tokunaga M, Takano Y, Togano K, Kito H and Ihara H 2003 *J. Low Temp. Phys.* **131** 1153

[74] Agterberg D F and Walker M B 1995 *Phys. Rev. Lett.* **74** 3904

[75] Schemm E R, Gannon W J, Wishne C M, Halperin W P and Kapitulnik A 2014 *Science* **345** 190

[76] Hirsch J E, Maple M B and Marsiglio F 2015 *Physica C* **54** 1